Eur. Phys. J. B **15**, 483–492 (2000)

THE EUROPEAN PHYSICAL JOURNAL B

EDP Sciences

A model for the self-organization of microtubules driven by molecular motors

B. Bassetti[1,a], M. Cosentino Lagomarsino[2], and P. Jona[3]

[1] Dipartimento di Fisica, Università di Milano, Via Celoria 16, 20133 Milano, Italy
[2] Università degli Studi di Milano, Dipartimento di Fisica, Fisica Teorica, Via Celoria 16, 20123 Milano, Italy
[3] Politecnico di Milano, Dipartimento di Fisica, Piazza Leonardo da Vinci 32, 20123 Milano, Italy

Received 4 August 1999 and Received in final form 24 November 1999

Abstract. We propose a two-dimensional model for the organization of stabilized microtubules driven by molecular motors in an unconfined geometry. In this model two kinds of dynamics are competing. The first one is purely diffusive, with an interaction between the rotational degrees of freedom, while the second one is a local drive, dependent on microtubule polarity. As a result, there is a configuration dependent driving field. Applying a molecular field approximation, we are able to derive continuum equations. A study on the solutions of these equations shows non-equilibrium inhomogeneous steady states in various regions of the parameter space. The presence and stability of such self-organized states are investigated in terms of entropy production. Numerical simulations confirm our analytic results.

PACS. 05.65.+b Self-organized systems – 64.60.Cn Order-disorder transformations; statistical mechanics of model systems – 87.16.Ka Filaments, microtubules, their networks, and supramolecular assemblies

1 Introduction

Using a theoretical physics approach, we introduce and analyze a stochastic model inspired by the self assembly process of the cytoskeleton.

The cytoskeleton can be seen as the "infrastructure" of eukaryotic cells, providing for both (dynamically evolving) spatial structure and internal transport processes that are fundamental for the cell itself and its role in a living organism [2]. We focus on questions concerning the statistical mechanics of this particular biological system, mainly its ability to assemble in a variety of symmetry-breaking phases, which are commonly believed to have non-equilibrium nature and are considered important for cell morphogenesis. The non-equilibrium forces that give rise to these phases are usually ascribed to both the so-called dynamic instability of microtubules (associated with a confining geometry, see for example [3]) and the action of molecular motors. Dynamic instability is a non-equilibrium polymerization/depolymerization process that enables microtubules or actin filaments to exert forces on confining surfaces such as the cell membrane. Molecular motors are a much studied family of proteins that are able to generate active motion on cytoskeletal filaments.

Numerical and *in vitro* experiments (some of which are called self-organization assays) [5–8], show that ensembles of microtubules and active motors can self-organize under proper conditions, and this ability is strictly linked to motor activity. In the *in vitro* self-organization assays, motors are typically found in soluble complexes and operate when two or more filaments are present; dynamic instability does not seem to be determinant.

In this paper we concentrate on the role of motor proteins and do not consider dynamic instability. In a previous article [9] we have theoretically shown that in motility assays, where motor proteins are adsorbed on surfaces and the "gliding" process of single microtubules is observed, rotational diffusion [1] leads to purely diffusive dynamics.

This finding brought us to investigate the breaking of rotational symmetry, in the form of pattern formation, as a many body effect. That is, we consider the excluded volume interaction of many filaments. This is different from cooperation of motor proteins that is typically investigated in the situation of muscle contraction; (see [10,25] for interesting recent examples of stochastic modeling in this context).

Concisely, our problem can be stated in terms of existence of inhomogeneous non-equilibrium steady states. From this viewpoint, our model is on the same level as many other models of non-biological systems, such as a fluid with convecting flow, or a non-equilibrium chemical reactor (this is true as long as we are not modeling the self-regulatory processes that take part in cell morphogenesis, see [4]).

What makes our choice distinct and particularly interesting for statistical mechanics is that the generalized force which keeps the system far from equilibrium is not,

[a] e-mail: bassetti@mi.infn.it

in general, a global field or some boundary condition, as is usually found in the literature on far from equilibrium systems, but a local release of energy associated with transport.

The model, which is a two-dimensional lattice spin system, is presented in Section 2.

In order to discover the relevant variables of the real system we explored different ways to implement its microscopic dynamics [11]. In this paper we limit the discussion to the simplest case we could find showing significant results.

This point needs some clarification. Our working hypothesis is that the relevant features of the system are the competition between diffusion and motor drive, together with excluded volume interactions. The aim of our investigation is not to reproduce in detail the mechanical features of the microscopic system but rather to analyze the behavior of averaged quantities. Many different dynamics can reproduce the right averages (we follow the concept of universality in statistical mechanics), so our objective is to find the essential features that a microscopic dynamics needs to have to reproduce the desired behavior. Of course this leaves many possibilities open to choose a microscopic dynamics and one has to be guided by considerations on experimental models. Such considerations are extremely useful to give an intuitive grasp on the interpretation of microscopic dynamics. Nevertheless, the rigorous justification of our microscopic model has to be sought in the results it gives for macroscopic, averaged observables.

All of the dynamics we developed are based on the competition between a diffusive process (when motors are detached from filaments or not active) and a driven-diffusive one (when motors are active), this means that they fall in the class of competing dynamics models [14,15].

In the system presented in this paper, the driven process is developed in a way that is resemblant to Schmittmann and Zia's driven diffusive systems [12,13]). This case is most easily interpreted in terms of many body motility assays, so we will stick to this interpretation throughout the paper. Unfortunately, we are not aware of any experiments of this kind focused on self-organization, so we dedicate Section 6 to discuss the possibilities of employing this microscopic dynamics for the experiment in reference [6] and the results we obtained with a different choice for the driven process, which seems more sound for this case.

In Section 3, starting from microscopic dynamics, we use a mean field approximation to derive a set of four discrete evolution equations for the system. We discuss the problems that arise when one considers the continuum limit of these equations in order to obtain a more at hand system of differential equations. In particular, the result of this limit is related to the characteristic times of the two competing dynamics.

Once we have obtained a set of differential equations on $\mathcal{R}^2$, we look for steady states in different regimes. In the two limiting cases of dominant diffusion and dominant drive, we find, respectively, the usual homogeneous Gibbs states and blocked phases; whereas, when the two dynamics are mixed, a new class of entropy-producing, phase-separated states emerges. By linear stability analysis, we find in parameter space the instability region of the homogeneous states.

Finally, in Section 5, the analytical results are compared with those obtained by numerical simulation. In order to tackle the problem of entropy production numerically, we apply some of the machinery related to the fluctuation theorem by Gallavotti and Cohen (reviewed in [16]), that has recently been established for stochastic dynamics [17–19].

2 Microscopic dynamics

We imagine that motors are adsorbed on a flat surface and can push the filaments as in motility assays. Our aim is to find a transition to self-organized, inhomogeneous states. Experiments of this kind, though in principle possible, have not been tried to our knowledge.

On the other hand, in the self-organization experiments described in [6,7], microtubule-associated motors are linked in bundles by some other proteins, and the bundles are in solution. Links of these experiments to our model will be discussed in Section 6.

We discretize space, time, and the orientation of the filaments. So we define a 2-dimensional square lattice Λ and we imagine that each lattice site is either empty or occupied by the center of mass of a filament. This corresponds to associate to each lattice site $x \in \Lambda$ a spin σ_x which takes the null value when the site is empty. The other possible values of the spins are determined by the discretization on the orientational degree of freedom. With these assumptions, microtubules are treated as rigid rods, and dynamic instability is neglected. The minimal choice is that spins take values in $\{+1, -1, +\mathrm{i}, -\mathrm{i}, 0\}$, corresponding to the four fundamental orientations of the filaments and to the empty site (see Fig. 1). Our results will show that this choice is significant.

The thermodynamic equilibrium properties of the system are determined entirely by its Hamiltonian H. We take

$$H = J \sum_{\substack{x,y \\ \text{n.n.}}} \sigma_x^2 \sigma_y^2 + K \sum_{\substack{x,y \\ \text{n.n.}}} \sigma_x^4 \sigma_y^4. \tag{1}$$

This is just the most generic form that H can take in our case, provided that the interaction is nearest neighbor.

Intuitively, the first coupling constant, $J < 0$, stands for an interaction between the directions of the rods (regardless of their orientations), and mimics excluded volume effects on directions. K, on the other hand, is sensitive to the presence or absence of the filaments.

The choice of a nearest neighbor Hamiltonian is connected to the problem of the filament length. From a purely geometrical point of view, if a is the lattice spacing, a filament of length L should interact with $\frac{L}{a}$ sites. On the other hand, we can do the statistical mechanics of this system after a preliminary coarse graining procedure.

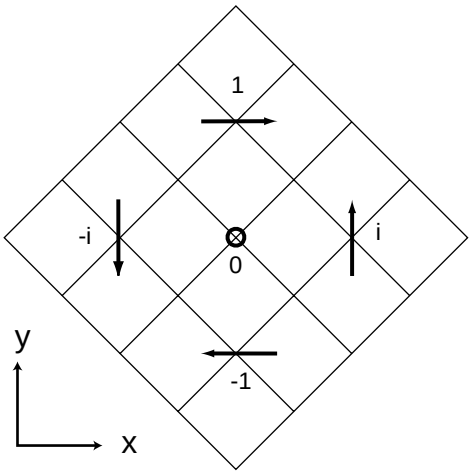

Fig. 1. Conventions adopted for lattice and occupation variables. Complex values of the spins are merely adopted to make our computational life easier. Microtubule directions are along the axes. Spins are 45° to lattice bonds so that interaction with all four nearest neighbors is symmetric.

This renders the Hamiltonian nearest neighbors, while the constants J and K keep memory of the original scale, becoming functions of the (mean) length L of the filaments (for example $J, K \sim L^2$, see [23]). The spin of each site takes the meaning of a cluster spin, so even though we speak of filaments as they were in 1:1 correspondence with our spins, this is merely a convention, because one spin may already be the result of mesoscopic averaging procedures.

From expression (1) it is easy to see that the statics of this model is equivalent to that of the 2-D Blume-Emery-Griffiths model with only two relevant coupling constants (see [20] for a complete mean-field analysis of the phase diagram). In fact, the effective levels reduce to three ($\sigma^2 = \pm 1, 0$), two of which are 2-fold degenerate. They correspond to the two possible directions (regardless of orientation) of the filaments and their absence.

Since external fields are absent, our Hamiltonian produces two kinds of spatially isotropic states, which are associated respectively with the well-known liquid/gas and isotropic/nematic transitions [20]. Note that the phases that the system can exhibit are related with the assumption on the discretization of the rotational degrees of freedom. A finer discretization could bring to a larger number of phases. However, the phases would all be spatially isotropic, causing little change in the problem of the transition to inhomogeneous states.

We now consider the time-dependent properties of the model. The evolution algorithm is made of two branches, the first of which is a diffusion and the second a driven diffusive process. Both processes take place in presence of the Hamiltonian H and include two kinds of elementary Monte Carlo moves:

- Nearest neighbor spin exchange (only effective when one of the two sites is empty) $\sigma_x \leftrightarrow \sigma_{x'} \quad x' \in \text{n.n.}(x)$ (Kawasaki dynamics).

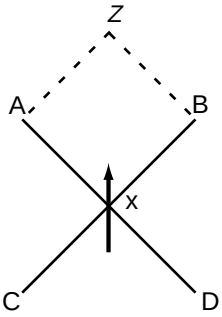

Fig. 2. Motor action. ΔH is shifted by $-E$ for Kawasaki exchanges with sites A and B, identified by the arrow head, and by $+E$ for exchanges with C and D.

- Local orientation $\sigma_x \neq 0 \rightarrow \sigma'_x \neq 0$ (Glauber dynamics).

In the diffusive steps, when the interaction with motors is not active, the two kinds of moves correspond respectively to translational and rotational diffusion of a microtubule.

The probability of accepting a move is a modified Metropolis

$$\mathcal{A} = \frac{1}{2}\left(1 + \tanh\frac{\Delta H}{2}\right).$$

We now "turn on" the interaction with motor proteins, and see what happens. What we assume is that motor drive will act on the translational diffusion of the centers of mass of the filaments, transforming it in a driven diffusion, and that rotational diffusion will be inhibited.

In order to model motor activity, we modify $\mathcal{A}$ in the same way that is commonly used in the context of driven diffusive systems [12]. That is, $\Delta H(\mathrm{C}, \mathrm{C}') \rightarrow \Delta H(\mathrm{C}, \mathrm{C}') \pm E(\mathrm{C})$ when configuration C is favorable for motor pushing forward or pulling back the filament (see Fig. 2). H can be taken to be the same as in (1). $E(\mathrm{C})$ is the driving field, and is proportional to the work done by the motors.

This way of modeling molecular motor driven dynamics contains a number of hypotheses. First of all, we suppose that the motors will push the microtubules every time they can. Secondly, the motors are spread with constant density and push one filament at a time (an intuitive assumption for motility assays; in Sect. 6 it will be discussed for the case of self-organization assays). Lastly, the motor action forces microtubules to preserve their orientations. The justification for this last hypothesis for a motility assay lies in the fact that as soon as two motors are attached to one filament, its direction is frozen except for the elastic fluctuations of its head and tail (see [9,26]).

The fact that the pushing of the motor is actually a diagonal translation may cause some perplexities. On the other hand, our dynamics is set up taking into account two degrees of freedom, translational and rotational, that are independent. So they have to be activated in different elementary moves. The overall motion springs from a sequence of such moves. In this view, motor action is just a bias in the translational dynamics. We also tested [11]

numerically a dynamics where motors push linearly (exchange is favored with site Z in Fig. 2) obtaining no qualitative change in the results (but this choice complicates our analytic mean field calculations because of the fact that translations involve next nearest neighbors).

We would like to make a final remark on the boundary conditions. We adopted periodic boundary conditions in our simulations.

The simultaneous presence of two competing dynamics, each one with its own characteristic time, makes it reasonable to expect (see [15]) that possible steady states have a non-equilibrium (non Gibbsian) nature regardless of the boundary conditions. This fact is confirmed by our mean field analysis.

When considering the dynamics of active motors alone, the condition above ceases to be valid and we are in the case of a four species driven system. One should keep in mind the following remark.

When $E \neq 0$, the resulting driving field depends on the space-time configuration of the system. As it arises from a modification of the Metropolis acceptation probability, each translational step of the microscopic dynamics automatically satisfies detailed balance with respect to the modified energy difference,

$$\frac{W(\mathrm{C}' \to \mathrm{C})}{W(\mathrm{C} \to \mathrm{C}')} = \frac{P_{\mathrm{eq}}(\mathrm{C})}{P_{\mathrm{eq}}(\mathrm{C}')} = \mathrm{e}^{\beta(\Delta H \pm E(\mathrm{C}))}.$$

However, in general, detailed balance is not satisfied for periodic boundary conditions [12]. For this reason, one can expect to observe inhomogeneous ("blocked") steady states even in the presence of the sole motor dynamics.

To sum up, the main features of the model are the following:

- It is a model with competing dynamics. Thus, the characteristic time scale ratio of the two dynamics plays an important role in its behavior [14].
- It is related to so-called multiple species driven systems [12,13,21], to which it reduces when Glauber-like dynamics (rotational diffusion) is not active and periodic boundary conditions are set.
- It can be interpreted as a reaction/diffusion model, in which four diffusing species, driven in four orthogonal directions, are subject to (equilibrium) chemical reactions controlled by the Ising Hamiltonian (1).

3 Mean field approximation and continuum equations

The dynamics we described in the preceding section defines a Markov process on the lattice Λ. The time-dependent probability of a configuration $\mathrm{C} = \{\sigma_x\}_{x\in\Lambda}$ is given by the master equation [15,22]

$$\frac{\mathrm{d}}{\mathrm{d}t}P(\mathrm{C},t) = (\tau_{\mathrm{p}}\mathbf{L}_{\mathrm{p}} + \tau_{\mathrm{a}}\mathbf{L}_{\mathrm{a}})P(\mathrm{C},t) \qquad (2)$$

where τ_{p}, τ_{a} are the characteristic times of the two dynamics. Physically, τ_{a} and τ_{p} represent a slow process with respect to the entire process of interaction between a motor and a filament. Therefore at the time scale we adopt, the dynamics is regarded as a diffusive or a driven one when a filament encounters on average a small or a large number of motors respectively.

$\mathbf{L}_{\mathrm{p}}$, $\mathbf{L}_{\mathrm{a}}$ are the generators of the evolution when motors are passive and active respectively. The operators contain the transition probabilities $W(\mathrm{C},\mathrm{C}')$ from configuration C to C′, which can be easily written down following the description of the model given in Section 2. For diffusive dynamics regulated by Hamiltonian (1) (switched off motors)

$$W(x|\mathrm{C}\to\mathrm{C}') = \delta_{\sigma_x,0}\delta_{\sigma_x,\sigma'_x} + \frac{1}{4}(1-\delta_{\sigma_x,0})$$
$$\times\sum_q \Big\{(1-\delta_{\sigma_{x+q},0})\frac{1}{3}(1-\delta_{\sigma'_x,0})(1-\delta_{\sigma'_x,\sigma_x})[\frac{1}{2}(1-\mathrm{Th}\frac{\Delta H}{2})]$$
$$+ (\delta_{\sigma_{x+q},0})\delta_{\sigma'_x,0}\delta_{\sigma'_{x+q},\sigma_x}[\frac{1}{2}(1-\mathrm{Th}\frac{\Delta H}{2})]\Big\}.$$

In the case of driven dynamics the corrections are that Glauber transitions (rotations) are inhibited, and $\Delta H(\mathrm{C},\mathrm{C}') \to \Delta H(\mathrm{C},\mathrm{C}') \pm E(\mathrm{C})$ when the configuration is such that the motors can do work (Fig. 2).

Instead of postulating, as is usually done [12], some mesoscopic equations on the basis of symmetries and physical considerations, we start from microscopic dynamics and develop a local mean field approximation. The main assertion of this approximation is that the probability of a configuration factorizes as

$$P(\sigma_x) = \prod_{x\in\Lambda} p(\sigma_x)$$

where $p(\sigma_x)$ is the most general single site measure:

$$p(\sigma_x) = \sum_I p_I\delta_{\sigma_x,I}; \quad \sum_I p_I = 1,$$

(I runs on all the possible values of the spin).

With these assumptions, the mean value of a function of n spins can be written

$$\langle F(\sigma_{x_1},\ldots,\sigma_{x_n})\rangle = \sum_{I_1,\ldots,I_n} F(I_1,\ldots,I_n)[p_{I_1}(x_1)\ldots p_{I_n}(x_n)].$$

We use this approximation to obtain the evolution equations of the first moments. Such discrete equations are sums of the mean values of some quantities computed in four different sites of the lattice, reaching next-next nearest neighbors. Namely, given a lattice versor $\mathbf{a}$, one has to consider the cluster containing both the nearest neighbors of x and those of $x+\mathbf{a}$. We get expressions that involve the parameters

- $H(x) = \langle 1-\sigma_x^4\rangle$ (density of holes);
- $M(x) = \langle\sigma_x^2\rangle$ (quadrupole moment; interpreted as the mean value of the net filament direction);
- $g(x) + \mathrm{i}f(x) = \langle\sigma_x\rangle$, identified with vector field $\mathbf{D}(x) = (g(x), f(x))$ (orientation of the filaments).

Using Taylor expansions we obtain the following equations:

$$\dot{H} = -\mathrm{div}[-\nabla H + JHM\nabla M - KH(1-H)\nabla H] - rE\,\mathrm{div}\,(H\mathbf{D}) \quad (3)$$

$$\dot{M} = \mathrm{div}[(H)^2\nabla\frac{M}{H} + JH(1-H)\nabla M - KHM\nabla H] + rE\,\mathrm{div}\,(H\hat{T}\mathbf{D}) - (1-r)(M + \mathrm{Th}(4JM)) \quad (4)$$

$$\dot{g} = \mathrm{div}[H^2\nabla\frac{g}{H} + JgH\nabla M - KgH\nabla H] + rE\partial_x[(1-H+M)H] - (1-r)g(1+\frac{1}{2}\mathrm{Th}(4JM)) \quad (5)$$

$$\dot{f} = \mathrm{div}[H^2\nabla\frac{f}{H} - JfH\nabla M - KfN\nabla H] - rE\partial_y[(1-H-M)H] - (1-r)f(1-\frac{1}{2}\mathrm{Th}(4JM)), \quad (6)$$

where $\hat{T}$ is the conjugate operator in R^2.

A continuum limit has been performed along an appropriate path in parameter space, so that one characteristic time and the lattice spacing a have been eliminated. Consequently, we are left with four significant (rescaled) parameters, J, K, E, r. The first two concern the equilibrium properties of the system, while the others are indicators of its being far from equilibrium.

r gives the relative weight of the two dynamics and is related to the ratio $\Gamma = \frac{\tau_\mathrm{p}}{\tau_\mathrm{a}}$ of the two characteristic times by the equality $r = \frac{1}{\Gamma+1}$. r is independent of the motor drive E; in fact, E only appears in association with r in the equations, so that we interpret the quantity rE as the non-equilibrium generalized force generated by the motor action.

In the equations above, r may be regarded as a free, phenomenological, parameter, as is not fixed by any assumption on our model.

Establishing the relationship between r and some underlying microscopic parameters, such as motor density and microtubule length, is a problem that falls beyond the reach of our model, and that requires a more detailed analysis of the physical system.

For motility assays, the analysis of Duke and others [26] specifies the microscopic process as a Markovian stochastic evolution of the number n of motor proteins attached to a microtubule. Following this work, one can identify (see [9]) τ_a with the mean first passage time for going from $n = 2$ (two attached motors) to $n = 1$ (one attached motor), and τ_p with the mean time in which a microtubule is attached to 0 or 1 motor, obtaining:

$$\tau_\mathrm{a} = \frac{L+2\bar{d}}{L+3\bar{d}}\frac{\bar{d}^2}{vL}\left(\mathrm{e}^{\frac{L}{\bar{d}}} - 1 - \frac{L}{\bar{d}}\right)$$

$$\tau_\mathrm{p} = \frac{L}{v} + \frac{2\bar{d}}{v}$$

where $\bar{d}$ is the mean distance covered by a filament before linking a motor; it can be related to the surface density of the motors and other physical parameters. v is the average speed of filaments, and L their length. This gives the expression for r

$$r = 1 - \frac{\frac{L^2}{\bar{d}^2}\left(1+3\frac{\bar{d}}{L}\right)}{\left(\mathrm{e}^{\frac{L}{\bar{d}}} - 1 - \frac{L}{\bar{d}}\right)}\,.$$

We have already said (page 485) that microtubule length enters through the parameters of our model. The above formula is a way to relate the filament length to the parameter r *via* independent, more detailed modeling.

Equations (3–6) have the structure of reaction-diffusion equations, with no source for H, as the filament number is fixed. The sources for M, g and f arise from the interaction between filament directions.

The existence of a source makes them different from other equations obtained in the same way for two-species driven diffusive systems [21,27]. Another difference is that in the latter case, having just two species and a field forcing in one spatial direction, mean field equations come out to be one dimensional, while ours are not. However, by the general consideration that patterns are usually lower-dimensional (see [28]), we expect that our solutions will depend on one spatial variable, as well. The following sections will provide more specific justifications of this fact.

4 Steady states and stability

A quick glance at our equations is sufficient to conclude that they always admit the homogeneous solution

$$H = \bar{H}$$
$$f, g = 0$$
$$M = \bar{M}$$

where, by definition of the parameters, $|\bar{M}| \le \bar{H}$, and $\bar{M}$ satisfies the Ising-like equation

$$\bar{M} + \mathrm{Th}(4J\bar{M}) = 0.$$

The above solution is the Gibbs equilibrium one when $rE = 0$.

It is interesting to notice that, when $E = 0$, even if $r \neq 0$, our equations can be derived from an equilibrium free energy; that is, they have the form $\dot{\mathbf{X}} = \frac{\delta F}{\delta \mathbf{X}}$, with F a suitable functional of the fields. In particular, equations (3, 4) are decoupled from equations (5, 6). The first two describe a relaxation process to the equilibrium phases of our model, while the others admit as a unique stationary state the null field $\mathbf{D} = 0$. These considerations cease to be true as soon as $E \neq 0$.

In fact, when $rE \neq 0$, non-zero irreversible currents for f and g arise:

$$J_g = rE\bar{H}(1-\bar{H}+\bar{M}) \quad (7)$$

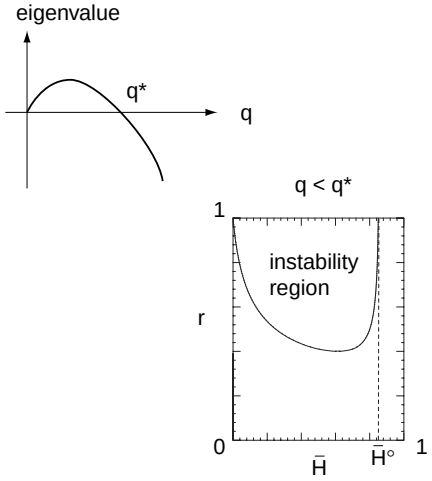

Fig. 3. Linear stability analysis results. q is the wave vector of the perturbation. For $q > q^*$ the solution is always stable (up). If $q < q^*$, E and M are fixed, the stability region looks like the one represented in the lower sketch.

and similarly for J_f. These stationary currents are the mirror of a nonzero entropy production which we can measure numerically (see Sect. 5), and, as with this last quantity, are linear in the non-equilibrium drive rE.

We perform linear stability analysis around this homogeneous solution (resumed in Fig. 3), to find out that the system, far from equilibrium, for perturbations of small wave vector, becomes unstable in a region of the $\bar{H}, r$ plane.

Our methods coincide with the ones in [28]. Current terms are kept to lowest order. q is the wave vector of the perturbation. The instability may arise only for perturbations of wave vector smaller than q^*. This implies that the size of the system must be at least of order $1/q^*$, or else the homogeneous solutions will be the only stable ones. For $q < q^*$ we find an instability if

$$\frac{\bar{H}(1-2\bar{H}+\bar{M})}{(1-\bar{H})(1-\frac{\bar{M}}{2})} > \frac{1-r}{r^2E^2}\,.$$

As can be seen from the picture, for low concentration of filaments and low r the system is always in a stable homogeneous state. The system may become unstable after r reaches a critical value r_c.

The next thing to do is to verify that this instability leads to the inhomogeneous solutions we expect. In doing this, we employ the same techniques used in [21,27], that is, successive substitutions leading to a nonlinear dynamical system for the variable H. Let's outline our procedure. By keeping terms to lowest order in the fields one has a hint at what the solutions look like. In this view, from equation (3) one obtains the relation

$$\nabla H = rEH\mathbf{D} + \dots \tag{8}$$

When $r \in (0,1)$ and the two dynamics are actually competing, Using (8) in equation (4) we can write an expansion of $M(x)$ around the Ising value $\bar{M}$

$$M = \bar{M} + \alpha[(1-\bar{M})\partial_x^2 H - (1+\bar{M})\partial_y^2 H] + \alpha^2 \dots \tag{9}$$

with

$$\alpha = \frac{1}{(1-r)(1+\frac{J}{\cosh^2(J\bar{M})})}.$$

The last step is to use these two results in equations (5, 6).

It is easy to acknowledge that the source terms for g and f, are equal to zero *iff* g and f themselves are. Thus, the two fields are tendentially brought to zero by the dynamics (Eqs. (5, 6)).

However, the decay times of f and g are very different. Precisely, they are determined by the sign of M. Accordingly, one of the two, say f, goes rapidly to zero while the other does not, so equation (6) allows studying the stationary states that depend on just one spatial variable, and we can substitute relations (8, 9) in equation (5) and obtain (similarly as in [21,27]) the ordinary differential equation for H

$$\left(\frac{\partial H}{\partial x}\right)^2 = AH^4 - r^2E^2H^3 + \frac{1}{2}r^2E^2(1+\bar{M})H^2 + BH - (1-r)\frac{2+\bar{M}}{6}H\log|H| \tag{10}$$

where A and B are constants of integration, related by the constraint that total density is fixed.

We find two classes of solutions of equation (10). The first are periodic functions, while the other are the stripe-like states shown in Figure 4.

Rigorously, we should perform a linear stability analysis around the solutions we find to make sure they are stable, and thus significant. Unfortunately, this is a very hard task, so we have to rely on the observation that in numerical simulations inhomogeneous states appear and are long lasting.

If we consider an unbounded system and impose the boundary condition that H has a constant value (interpreted as the background density of holes) at $\pm\infty$, the constants of integration are fixed, and the only solution

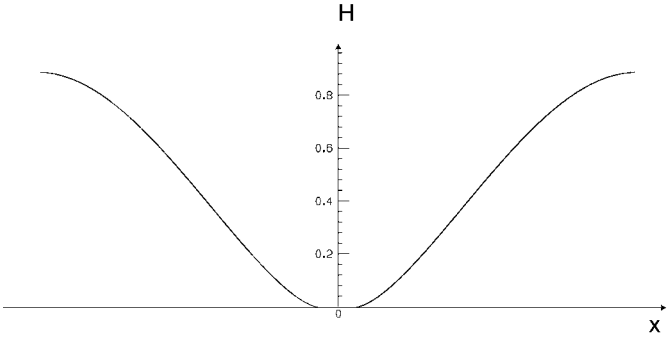

Fig. 4. Plot of a solution of equation (10) obtained with the boundary condition $H(x) \longrightarrow H_1$ as $x \to \pm\infty$, which, given the total density, fixes the width of the stripe.

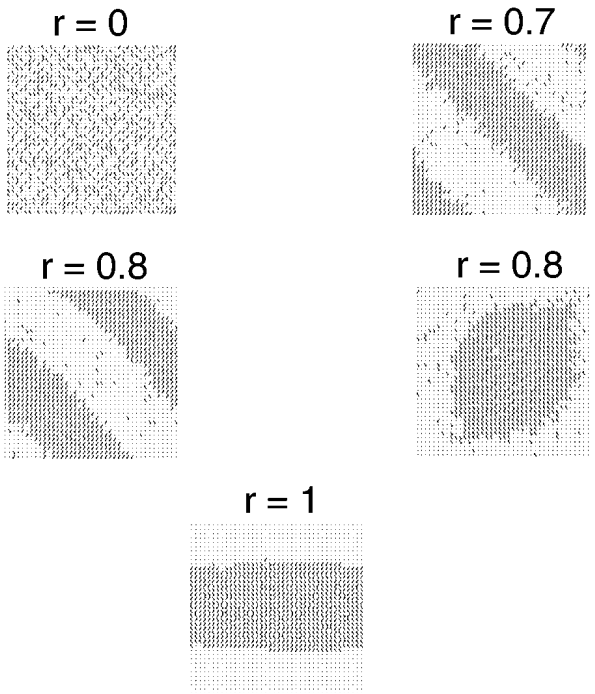

Fig. 5. Steady states obtained with our simulations for $J = 1$, $K = 1.5$, $E = 8$ and different values of r. The case $r = 0$ is the equilibrium state, and the system is not sensitive to the value of E. For $r = 0.7$ a stripe-like pattern is clearly identifiable. As r becomes closer to 1, droplet-like metastable states become more and more long lasting. For $r = 1$ we obtain blocked states. These results do not change sensibly as long as $J > 0$ and J, K are significantly lower (about one order of magnitude) than E. K can be positive or negative. Note that, for $r = 1$ the system is disordered in orientation.

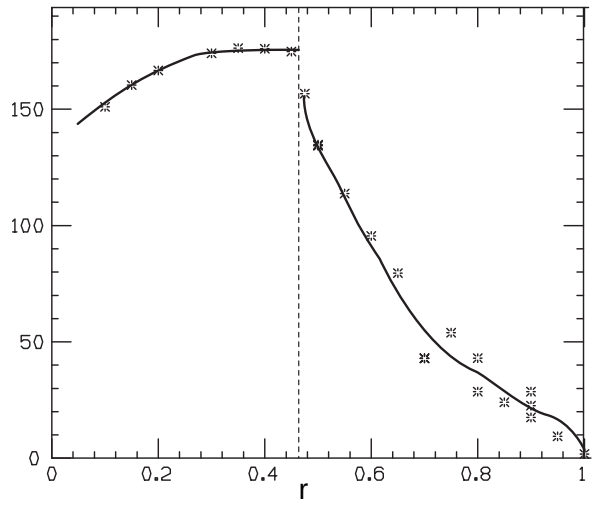

Fig. 6. Accepted translations per sweep at the steady state, mean value. The parameter is plot *versus* r, and E is fixed ($J = 1$, $K = 1.5$, $E = 8$). The slope of the curve represents the mobility, which, after reaching the saturating value of zero has a jump to negative values, meaning that an increasing drive inhibits translations. The jump in this parameter corresponds to the critical value for r. Doubling E determines a change in the calculated points of less than four percent (this is also valid for Figs. 7–9).

that we get is stripe-like. Differently from the ones found in the literature [21], our stripe-like solutions are characterized by the fact that H may reach the null value. So that there exist lines along which the density reaches its maximum value, compatibly with excluded volume. Along the same lines we find a discontinuity jump of the orientation field $\mathbf{D}$, whereas M fluctuates around the Ising value $\bar{M}$ modulated by the second derivatives of H. (Notice that, at this stage, the constraint that M must always be lower than H has to be implemented; we verify that it is satisfied for suitable values of J.) This behavior is confirmed by the results of our numerical simulations. For comparison, in Figure 5 are shown some snapshots of stationary states taken from our simulations.

Finally, we want to note that, for $r = 1$ (and $E \neq 0$), the four species are always simultaneously present and conserved, so the expansion (9) around the Ising value of M ceases to be significant, and is substituted by the relation

$$\nabla \frac{M}{H} = E\hat{T}\nabla \frac{1}{H} + \dots$$

In this formula the presence of the conjugate operator $\hat{T}$ imposes that the solutions depend on just one spatial variable, in agreement with a pure multi-species driven diffusive system, and we find so-called "blocked" states present in the literature.

5 Simulations. Entropy production

We perform simulations at fixed total density equal to 1/2 on a 40×40 square lattice. Monte Carlo time unit τ corresponds to 1600 moves, or one lattice sweep. E is typically one order of magnitude greater than J and K.

Among the parameters we examine are the mean values of M and $\mathbf{D}$, and the mean number of accepted rotational and translational Monte Carlo moves (per sweep). The latter quantities measure the relative mobility of the system, that is, how much a state is "blocked" (see Figs. 6 and 7).

In order to calculate these means, data are sampled each $10^3\tau$. Total running time is about $10^6\tau$. The time to reach a steady state goes from 10^4 to $10^5\tau$. Inhomogeneous steady states typically arise for great enough values of rE and have the form of a stripe either orthogonal or oblique with respect to the direction chosen by the filaments. An alternative state is shaped like a droplet (of arrows with the same direction). This last state is metastable for intermediate values of r, but its stability time diverges as $r \to 1$ (see Fig. 5).

To analyze these states, we pay particular attention to the entropy production and the structure factor.

Following Lebowitz and Spohn [18], we define the entropy production at the stationary state as

$$\frac{\mathrm{d}}{\mathrm{d}t} S_{\mathrm{irr}} = \frac{\mathrm{d}}{\mathrm{d}t} S_{\mathrm{flux}} = \frac{1}{t} \langle W(t) \rangle$$

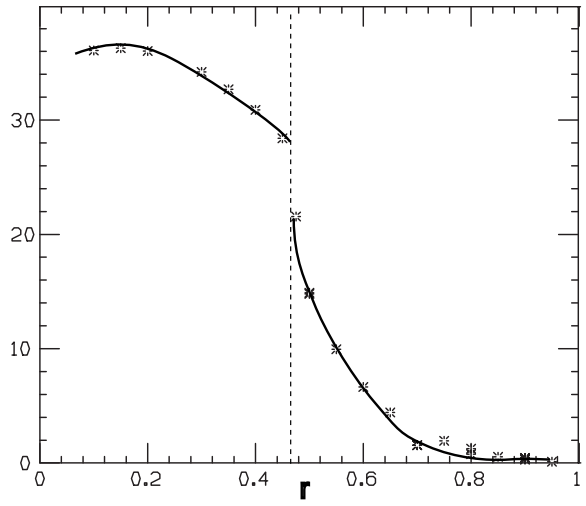

Fig. 7. Mean value of accepted rotations per sweep *versus* r at the steady state ($J = 1$, $K = 1.5$, $E = 8$). A decided drop of this parameter is observable at critical r.

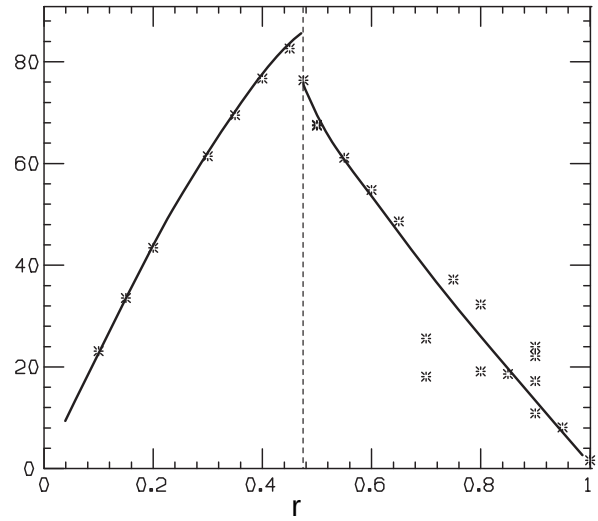

Fig. 8. Entropy production at the steady state as a function of r ($J = 1$, $K = 1.5$, $E = 8$). After the parameter attains its maximum, there is a drop and the system begins to structure. In the high r region the situation is more confusing because of the appearance of metastable states. In fact droplets usually produce less entropy than stripes. When $r = 1$, entropy production of the steady states appears to be practically zero, even though the states are not absorbing, because the microscopic dynamics is, in principle, active. This effect is a consequence of the fact that the driving field E is very strong.

with

$$W(t) = E \int_0^t \sum_{i=1}^{4} \sum_{\text{bonds}} J_{\text{bond},i}(s)\mathrm{d}s$$

where $J_{\text{bond},i}$ is the net current of the ith species along the bond in the driven dynamics, and the above integral is just a sum over Monte Carlo times.

With this definition, we identify two distinct regimes (Fig. 8).

In the first one, characterized by low r, a class of homogeneous entropy producing steady states is observable, and entropy production increases almost linearly with r (see Sect. 4).

In the second regime inhomogeneous steady states appear, and entropy production drops. The critical value of r that separates these two behaviors is also evident from the graphs of mean accepted moves per sweep (Figs. 6 and 7). We estimate this value to be $r_c \simeq 0.45$. Considering the discontinuities in the parameters, we believe that the transition is of the first kind.

On the other hand, the structure factor is defined as

$$S(k) = \langle |G(k)|^2 \rangle$$

with

$$G(k) = \frac{1}{L} \sum_x \sigma_x^4 \mathrm{e}^{2\pi \mathrm{i} k \cdot x}.$$

In particular, we observe the values assumed by $S(k)$ in correspondence with wave vectors k that are sensitive to stripe-like states in various directions; namely $k = (0,1), (1,0), \frac{\sqrt{2}}{2}(1,1), \frac{\sqrt{2}}{2}(1,-1)$. If suitably normalized, these quantities take the value of unity when the stationary state is a stripe in a well-defined direction; typical values for droplet-like states are around 1/2.

Notice that time averaging of $|G(k)|^2$ may be meaningless if the system explores a number of different inhomogeneous steady states, so one has to be very careful about the state being stable.

Figure 9 is a plot of the structure factor of the steady state as a function of r. In the high r region, metastable states are subject to a slowing down of the dynamics and become long lasting. This is reflected by the two distinct behaviors of the structure factor that can be seen in the picture (see also Fig. 8).

To sum up, our numerical studies confirm the results of mean field analysis, and reveal a more intricate phenomenology for higher values of r. Due to the appearance of a slowing down in the dynamics, we suspect the existence of a second phase transition in this region, but more work is needed. In particular, a finite size scaling analysis could be important.

6 Links to self-organization assays

We proceed by suggesting a possible interpretation of the microscopic model in terms of self-organization assays (mainly Ref. [6]).

In doing this, there are a few main issues to address. First of all, our spins are driven one at a time whereas filaments need to be at least two to be driven by the cross-linking soluble motor complexes of [6]. Second, motor complexes do not have a fixed position, but can diffuse. Third, as the cross-links between filaments can produce a torque,

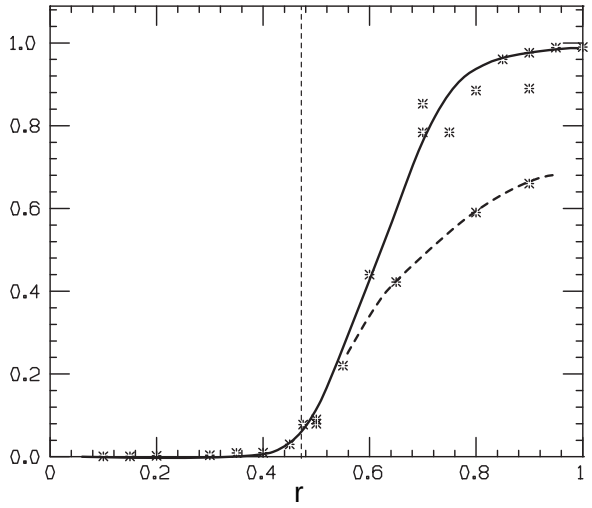

Fig. 9. Structure factor as a function of r ($J = 1$, $K = 1.5$, $E = 8$). This quantity starts to rise when r reaches its critical value. The dashed line represents metastable droplet-like states, which become long lasting as r increases, and stable for $r = 1$. The solid line stands for stripe-like states, regardless of their orientations.

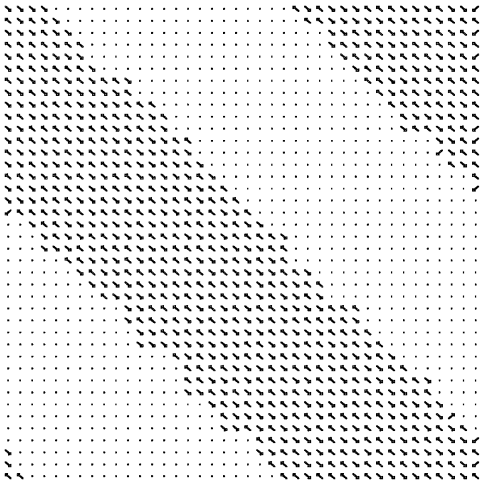

Fig. 10. Stripe-like stationary state for the dynamics mimicking self-organization assays. The values of the parameters are $J = 1$, $K = -5$, $E = 2$, $r = 1/2$.

a new question arises: do we need to take into account a driven rotational dynamics?

Dealing with the first two issues is quite a simple matter.

In particular, the first one affects the elementary move of the motors. We have tested a different dynamics for motor drive [11] which is more intuitively connectible with the experiments in question. Referring to Figure 2, the move of a motor is favoured by the field $E(\mathrm{C})$ if the sites A and/or B are filled, and is an exchange with the next nearest neighbor Z. Numerical results show the emergence of inhomogeneous states and the same qualitative behavior as the ordinary model. New kinds of self-organized states, as the stripe parallel to filament direction of Figure 10 appear. The continuum mean field theory becomes a bit more complicated, due to the appearance of terms in the powers of $(1-H)$ in our system of equations. These terms come from the need of a filled neighbor for a translation. Nevertheless, the identified solutions remain valid in the limit of high filament density.

As to the second issue, at the scale we consider, motors act as a random field and it is not relevant whether this is a result of Brownian motion or of a static configuration of the motors.

The third question is more essential and involves the role of rotational driven dynamics in the process of self-organization.

The fact that the forcing torque privileges the rotational moves aligning the filaments does not affect the nature of the stationary states. In fact, in our ordinary model, inhomogeneous states arise thanks to the joint effect of the driven translations and the aligning due to the coupling J. So the torsional drive is not in competition with equilibrium thermodynamics and can be absorbed in the coupling constants J and K, provided the system exhibits orientational order. Only an analysis of the times of relaxation could distinguish between the two behaviors.

Finally, the task of connecting the effective parameters of our model with the microscopic ones can be achieved with microscopic modeling of the kind of reference [26], specifically oriented on self-organization assays.

7 Conclusion

We have introduced a model of non-equilibrium statistical mechanics whose most interesting feature is the fact that the generalized force is a dynamic configuration dependent field. This feature has been inspired by the action of molecular motors on cytoskeletal filaments, so we have made quantitative effort throughout the paper to interpret our model in terms of systems that involve these objects.

Through analytic (mean field) approach and simulations, we have found evidence for a non-equilibrium phase transition to inhomogeneous states. We were able to see that these inhomogeneous steady states are genuinely far from equilibrium, checking their microscopic currents and entropy production. This results may be seen as a theoretical evidence that a local drive in competition with diffusion and excluded volume effects are sufficient to reach self-organized states.

Work in progress on some variations of the model described in this paper make us confident on the generality of this statement. We already mentioned briefly two of these variations (pages 486 and 491). Other numerical experiments have been tried for quasi three-dimensional geometries, that is, allowing filaments to cross each other when diffusing with translations, and different moves for motor action, all showing the emergence of inhomogeneous stripe-like states.

More work is needed to understand fully the statistical mechanical properties of our model. In particular, we are working on three issues.

First of all we want to perform a more careful analysis of the high r region, aiming to understand the nature of the stripe-like and droplet-like states and their relation with the finite size of the lattice.

Secondly, we would like to know if the role played by the field M is the same when one has a less radical discretization of microtubule directions, for example if $\sigma \in S^1$.

Lastly, the dynamical properties of the relaxation of this model to its stationary states are fully undiscovered. In particular, an analysis of this kind could be useful to understand the role played by torsional drive in dynamics resembling self-organization assays.

References

1. To avoid misunderstandings, we will use the word direction intending it as the property of a line with no arrows, *i.e.* an angle θ between 0 and π. With the word orientation, instead, we will identify an arrow on this line, *i.e.* a $\pm$ sign for θ.
2. J.D. Watson *et al.*, *The Molecular Biology of the Cell* (Garland, New York, 1994).
3. T.E. Holy *et al.*, Cell Biology **94**, 6228 (1997).
4. M. Kirschner, M. Mitchison, Cell **45**, 329 (1986).
5. R. Heald, Nature **382**, 420 (1996).
6. F.J. Nédélec *et al.*, Nature **389**, 305 (1997).
7. T. Surrey *et al.*, Proc. Natl. Acad. Sci. USA **95**, 4293 (1998).
8. F. Gibbons, Ph.D. thesis, CIRCS at Northeastern Univ., Boston, 1998.
9. M.R. Faretta, B. Bassetti, Europhys. Lett. **41**, 689 (1998).
10. F. Julicher, J. Prost, Phys. Rev. Lett. **78**, 4510 (1997).
11. M. Cosentino Lagomarsino, Thesis, Università Statale di Milano, Milan, 1999.
12. B. Schmittmann, R.K.P Zia, *Phase Transitions and Critical Phenomena*, edited by C. Domb, J.L. Lebowitz (Academic, New York, 1995), Vol. 17.
13. B. Schmittmann, R.K.P Zia, Phys. Rep. **301**, 45 (1998).
14. J.F.F. Mendes, E.J.S. Lage, Phys. Rev. E **48**, 1738 (1993).
15. P.L. Garrido *et al.*, Phys. Rev. A **40**, 5802 (1989).
16. G. Gallavotti, Chaos **8**, 384 (1998).
17. J. Kurchan, J. Phys. A **31**, 3719 (1998).
18. J.L. Lebowitz, H. Spohn, J. Stat. Phys. **95**, 333 (1999).
19. C. Maes, preprint (1998).
20. D. Mukamel, N. Blume, Phys. Rev. A **10**, 610 (1974).
21. D.P. Foster, C. Godréche, J. Stat. Phys. **76**, 1129 (1993).
22. Y. Prigogine, G. Nicolis, *Self Organization in Nonequilibrium Systems* (Wiley, New York, 1977).
23. L. Onsager, Ann. N.Y. Acad. Sci. **51**, 627 (1949).
24. J. Zinn-Justin, *Quantum Field Theory and Critical Phenomena* (Oxford Univ. Press, 1989).
25. A. Vilfan *et al.*, preprint, Technische Univ. Munchen, 1998.
26. T. Duke *et al.*, Phys. Rev. Lett. **74**, 330 (1995).
27. B. Schmittmann *et al.*, Europhys. Lett. **19**, 19 (1992).
28. M.C. Cross, P.C. Hohemberg, Rev. Mod. Phys. **65**, 2 (1993).